



Contents lists available at ScienceDirect

## Composites Science and Technology

journal homepage: [www.elsevier.com/locate/compscitech](http://www.elsevier.com/locate/compscitech)

# Multi-walled carbon nanotube/nanostructured zirconia composites: Outstanding mechanical properties in a wide range of temperature

Mehdi Mazaheri<sup>a,\*</sup>, Daniele Mari<sup>a</sup>, Zohreh Razavi Hesabi<sup>b</sup>, Robert Schaller<sup>a</sup>, Gilbert Fantozzi<sup>c</sup>

<sup>a</sup> Ecole Polytechnique Fédérale de Lausanne (EPFL), Laboratoire de Physique de la Matière Complexe (LPMC), CH-1015 Lausanne, Switzerland

<sup>b</sup> School of Material Science and Engineering, Georgia Institute of Technology, Atlanta, GA 30332-0245, United States

<sup>c</sup> Laboratoire MATEIS, UMR 5510 CNRS, Institut National des Sciences Appliquées de Lyon, 69621 Villeurbanne Cedex, France

## ARTICLE INFO

## Article history:

Received 11 November 2010

Received in revised form 19 January 2011

Accepted 23 January 2011

Available online xxxx

## Keywords:

A. Ceramic–matrix composites (CMCs)

A. Carbon nanotubes

B. Mechanical properties

B. Creep

Mechanical spectroscopy

## ABSTRACT

Multi-walled carbon nanotube (MWCNT)/nanostructured zirconia composites with a homogenous distribution of different MWCNT quantities (ranging within 0.5–5 wt.%) were developed. By using Spark Plasma Sintering we succeeded in preserving the MWCNTs firmly attached to zirconia grains and in obtaining fully dense materials. Moreover, MWCNTs reduce grain growth and keep a nanosize structure. A significant improvement in room temperature fracture toughness and shear modulus as well as an enhanced creep performance at high temperature is reported for the first time in this type of materials. To support these interesting mechanical properties, high-resolution electron microscopy and mechanical loss measurements have been carried out. Toughening and creep hindering mechanisms are proposed. Moreover, an enhancement of the electrical conductivity up to 10 orders of magnitude is obtained with respect to the pure ceramics.

© 2011 Elsevier Ltd. All rights reserved.

## 1. Introduction

Ceramics are the best candidates for high temperature mechanical applications, because of strong covalent bonds that limit dislocation slip and therefore plastic deformation in comparison with metallic materials [1]. However, with increasing temperature other thermally activated mechanisms such as grain boundary sliding [2] accommodated by diffusional creep lead to time dependent plastic or even superplastic deformation [3,4]. Such an effect may be desirable for forming industry but in general it should be avoided for structural applications [5]. Therefore, many efforts have been conducted to pin grain boundaries at high temperature [1,6–9]. Owing to their extraordinary mechanical properties, carbon nanotubes (CNTs) [10] have recently attracted some attention as grain boundary pinners in ceramics [11–14]. However, because of difficulties in obtaining a homogenous distribution of CNTs throughout the matrix, CNTs damage during high temperature processing and weak interfacial bonding between CNTs and ceramic grains the mechanical properties of CNT-ceramic composites were in many cases disappointing [13,15–21]. A few reports also show an improvement in indentation fracture toughness [22] and contact

damage resistance of CNTs reinforced ceramics [23–25]. However, the benefits are still controversial [23] and the toughening mechanisms of this class of materials are not well understood [26]. Moreover, most researchers use the simple indentation test to measure the toughness, which may not be a valid test in the case of these composites [25].

In the present study, homogenous 3 mol% yttria stabilized zirconia (3YSZ) reinforced by different weight percentage of multi-walled carbon nanotubes (MWCNTs) were processed by Spark Plasma Sintering. High resolution transmission electron microscopy (HR-TEM) analysis revealed the efficiency of Spark Plasma Sintering (SPS) in the fabrication of nearly full-dense nanostructured composites without oxidation and any detrimental effect on MWCNT integrity. High resolution scanning electron microscopy (HR-SEM) and TEM showed that the distribution of MWCNTs was homogeneous and they were mostly located at zirconia grain boundaries. The efficiency of MWCNTs in grain boundary pinning at high temperature was investigated by mechanical loss spectroscopy and creep tests at low stress. The effect of MWCNTs on fracture toughness was measured by single-edge V-notch beam method and the results were compared with those obtained by indentation. Electrical conductivity was measured in order to assess the contiguity of the CNT network. We demonstrate that the presence of MWCNT substantially improves contradictory properties such as the room temperature toughness and hardness and the high temperature creep resistance.

\* Corresponding author. Tel.: +41 21 6933389; fax: +41 21 6934470.

E-mail addresses: [mehdi.mazaheri@epfl.ch](mailto:mehdi.mazaheri@epfl.ch), [mmazaheri@gmail.com](mailto:mmazaheri@gmail.com) (M. Mazaheri).

**Table 1**

Sintering temperature and characteristics of sintered 3YSZ/MWCNTs nanocomposites in comparison with monolithic zirconia.

Material composition	Sintering temperature (°C)	Fractional density (%)	Grain size (nm)
3YSZ	1250	99.3	145
3YSZ/0.5 wt.% CNT	1250	98.9	131
3YSZ/1.5 wt.% CNT	1250	98.5	121
3YSZ/3 wt.% CNT	1300	98.7	109
3YSZ/5 wt.% CNT	1350	98.4	96

## 2. Materials and methods

### 2.1. Materials

Commercially available high purity 3 mol% yttria stabilized zirconia (3YSZ) powder (Tosoh Co., Japan) and multi-walled carbon nanotubes (Arkema, France) were selected as starting powders. Scanning electron microscopy (SEM, XLF-30, Philips, Netherlands) examinations show that the raw powder (covered with a thin layer of carbon) is constituted of spherical nanoparticles having an average diameter of about 70 nm. The MWCNTs used in this study are the commercially available grade Graphistrength C-100 by Arkema (France). They were synthesized by catalytic chemical vapor deposition. They have a length of around 20  $\mu\text{m}$  and a diameter of about 10–20 nm.

### 2.2. Processing

3YSZ powder with 0, 0.5, 1.5, 3 and 5 wt.% MWCNTs, were mixed by attrition milling with zirconia balls for 24 h. In order to obtain full-dense nanostructured composites (>98% of theoretical density TD), to retain the zirconia grains in nano-scale and avoid damage of nanotubes, the samples were processed by Spark Plasma Sintering (SPS, FCT GmbH, Germany) under vacuum at different sintering temperatures (Table 1). The composite powders were loaded into a graphite die (40 mm inner diameter) and a sheet of graphite paper was placed between the powders and die/punches for easy specimen removal. The heating rate, soaking time and applied pressure during SPS were 50 K min<sup>-1</sup>, 2 min and 50 MPa, respectively. The densities of sintered samples were determined by Archimedes method in deionized water. The theoretical densities of the composites were calculated according to the rule of mixtures. The density of graphite (2.25 g cm<sup>-3</sup>) has been used for MWCNT. Microstructural observations of sintered composites were carried out on the fracture surface and polished surface (with a diamond paste up to 0.05  $\mu\text{m}$ ) of carbon-coated specimens by HR-SEM (HR-SEM, FEI-SFEG, Philips, Netherlands). The average

grain size of the sintered compacts was determined by the linear intercept method on polished surfaces [27]. Analytical transmission electron microscopy (TEM, CM-20, Philips, Netherlands) and high-resolution electron microscopy (HR-TEM, CM-200, Philips, Netherlands) was made with a field emission gun operating at 200 kV on electron transparent area. TEM Specimens were prepared by tripod polishing method, followed by ion-milling.

### 2.3. Mechanical and electrical testing

Indentation tests were carried out with a diamond Vickers indenter under 20 kg load with a dwell of 20 s on the carefully polished surfaces. The fracture toughness was calculated by Antis equation [28]. The crack lengths were measured immediately after indentation using a calibrated optical microscope. At least 10 valid measurements were carried out for each sample and averaged. Bar (4 × 3 × 30 mm<sup>3</sup>) specimens were used for SEVNB fracture toughness measurements using the standard method. The notch preparation was made using a standard procedure [29]. The V-notch width was between 20 and 30  $\mu\text{m}$ . The specimens were bended using 4 point bending fixture with inner and outer span of 10 and 20 mm, respectively.

Conventional compressive creep tests were performed on specimens with size 3 × 3 × 8 mm<sup>3</sup> under vacuum and at constant stress of 6 MPa at 1600 K. Mechanical spectroscopy measurements were carried out in an inverted forced torsion pendulum, working at subresonant frequency. Samples of the size 25 × 1 × 4 mm<sup>3</sup> were excited in torsion and the deformation of the samples was detected by an optical cell. The measurements were performed under a high vacuum (10<sup>-3</sup> Pa) as a function of temperature in the range of 300–1600 K. The mechanical loss, tan( $\phi$ ), and the shear modulus,  $G$ , were measured from phase lag and the amplitude ratio between stress and strain signals, respectively. The amplitude of the applied cyclic stress during measurements was about 6 MPa. Shear dynamic modulus of composites with size 1 × 4 × 35 mm<sup>3</sup> was measured at room temperature in a free torsion pendulum. The electrical conductivity of composite with size of 2 × 2 × 10 mm<sup>3</sup> was measured at room temperature by a 4 point probe setup.

## 3. Results

### 3.1. Composite processing

Fig. 1 shows HR-SEM and bright field TEM image of mixed zirconia nanopowder with 5 wt.% (~12.5 vol.%) MWCNTs. Disentangled MWCNTs are well dispersed among zirconia nanopowder. No evidence of CNTs damage and agglomeration can be observed.

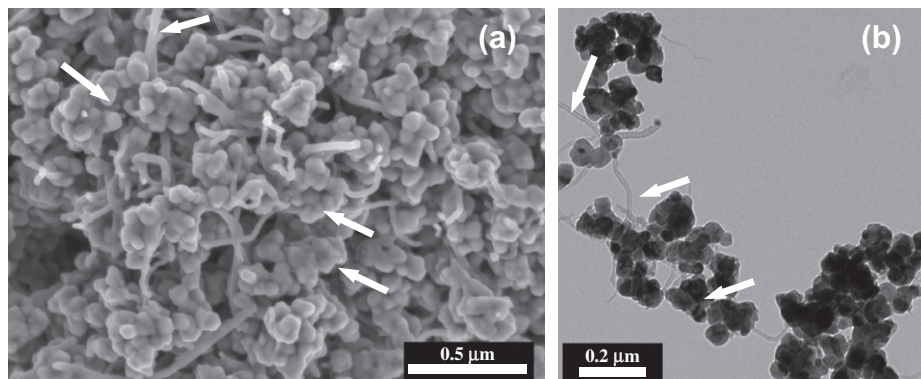


**Fig. 1.** HR-SEM (a) and bright field TEM (b) picture of 3YSZ nanopowder mixed with 5 wt.% MWCNTs after wet mechanical blending (arrows indicate nanotubes).

As seen in Fig. 1b, the unique flexible nature of CNTs makes them bend and pass through space between nanopowders or wrap around them. The same features were observed in composite powders with various amounts of MWCNTs.

Table 1 summarizes the sintering temperatures and characteristics (density and grain size) of sintered nanostructured composites and monolithic zirconia. Nearly full-dense structures ( $\rho > 98\%$  theoretical density) were obtained by SPS processing. As MWCNTs suppress densification to some extent [30], with an increase of MWCNTs content, higher sintering temperature must be employed. Nevertheless, the short SPS soaking/lower sintering temperature (Table 1) in comparison with conventional sintering [31] and hot-pressing [21,32] is the key to preserve the MWCNTs in the sintered composites [23,24,33]. Interestingly, though the highest sintering temperature was employed for zirconia reinforced with 5 wt.% MWCNTs, the final microstructure exhibits the smallest grain size. Therefore, MWCNTs substantially reduce grain growth and should also be able to pin grain boundaries and reduce their mobility during creep.

Fig. 2 shows a SEM picture of a fracture surface of 3YSZ/5 wt.% MWCNT and a TEM image of the composite microstructure after SPS. As seen in Fig. 2a, a fairly homogenous distribution of MWCNTs in the nanostructured zirconia matrix can be observed. Moreover, MWCNTs pull-out is apparent in the fracture surface. The length of pulled out fibers is not longer than 200 nm. The TEM image of as-sintered 3YSZ/5 wt.% MWCNTs (Fig. 2b) shows a homogenous grain size distribution and a random distribution of MWCNTs mostly located at grain boundaries and surrounded by the zirconia grains. HR-TEM of as-sintered 3YSZ/5 wt.% MWCNTs (Fig. 2c) reveals clean interfaces between CNTs and zirconia grains. Random orientation of MWCNTs by cross section and longitudinal section embedded between zirconia grains can be observed. No interlayer or amorphous carbon layer was detected and the fringe

spacing of 0.34 nm is typical of graphite [34], which shows that what is observed here is a true CNT section.

### 3.2. Room temperature properties

Fig. 3 represents some interesting properties obtained from MWCNTs reinforced zirconia nanostructured composites. First, a significant increase in indentation fracture toughness (Fig. 3a) is found with increasing CNT content accompanied with a slight but steady increase in the hardness (Fig. 3b). The indentation fracture toughness of 3YSZ reinforced by 5 wt.% MWCNTs reached  $\sim 11 \text{ MPa m}^{1/2}$ , which doubles that for monolithic 3YSZ. The fracture toughness was also measured by the single edge V-notch beam (SEVNB) method and is superimposed on data obtained by indentation showing that SEVNB fracture toughness also increases with MWCNTs amounts. The electrical conductivity as a function of MWCNT concentration is presented in Fig. 3c. A significant enhancement in the electrical conductivity, varying in orders of magnitude, is observed with MWCNT addition. This is not surprising and was already observed in different ceramics [35–37]. Long, thin and electrical conductive nanotubes create an interconnected percolation network through an insulating matrix.

### 3.3. High temperature properties

Fig. 4a shows the effect of MWCNTs on the creep strain of zirconia matrix nanostructured composites measured at low stress (6 MPa). In general, the curves indicate a typical strain-hardening creep curve, i.e. strain increases and the strain rate decreases with time. Obviously, creep is strongly reduced in the presence of MWCNTs even with the addition of a small amount of MWCNTs (0.5 wt.%). With higher amounts of MWCNT (1.5 wt.%), creep is even suppressed after a certain incubation time. More

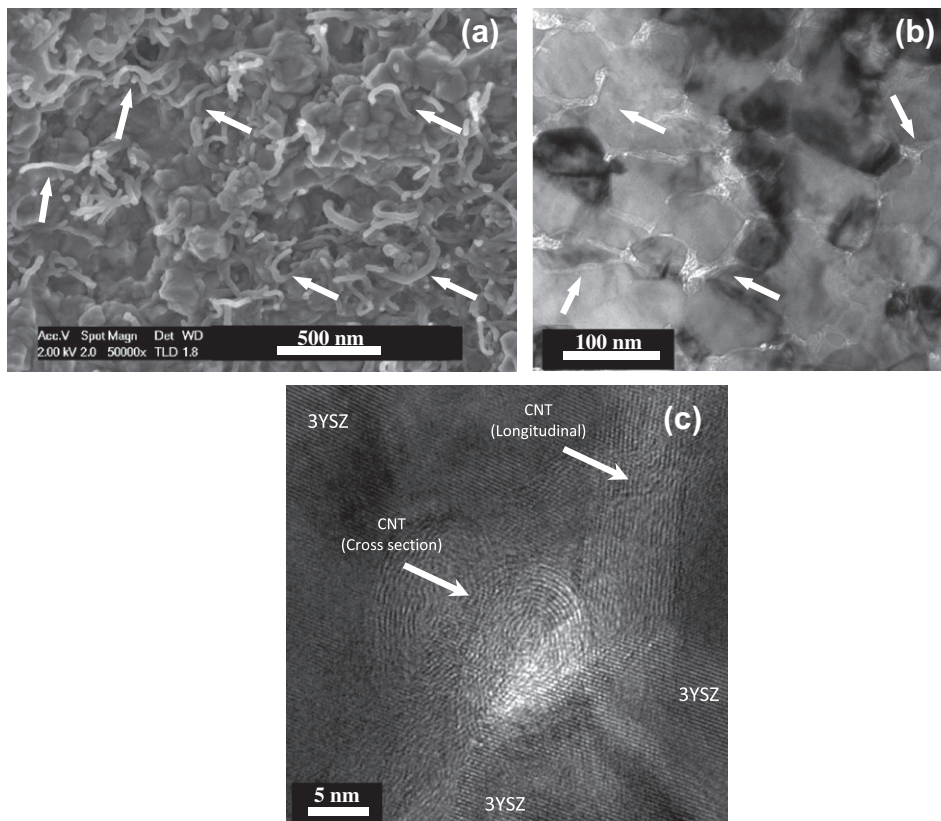
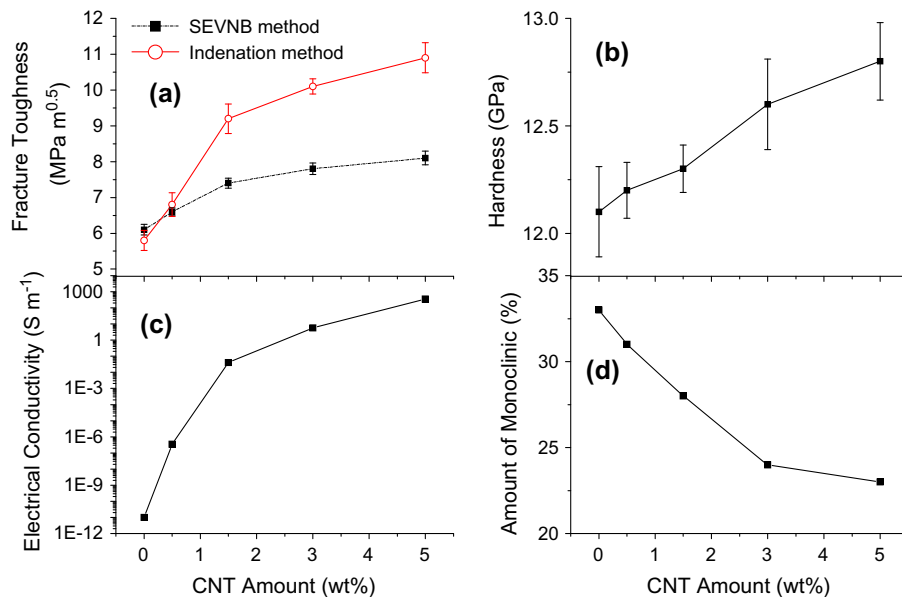
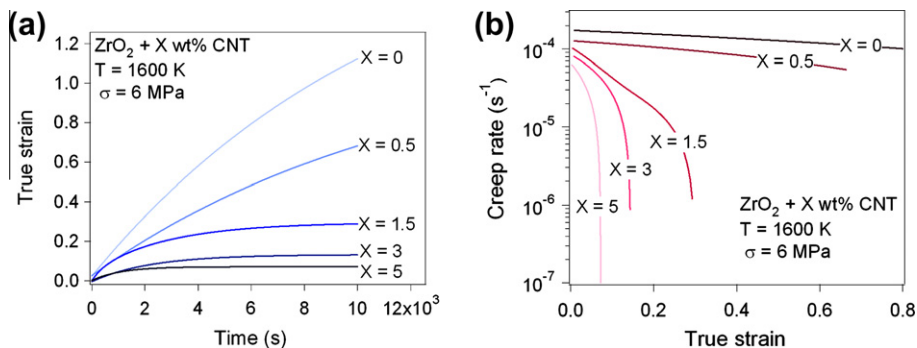


Fig. 2. HR-SEM picture of fractured surface (a), TEM image of as-sintered sample (b) and HR-TEM of interface between MWCNTs and zirconia grains (c).





**Fig. 3.** Fracture toughness (a), Vickers hardness (b), electrical conductivity (c) and amount of stress-induced monoclinic phase in fracture surface of the nanocomposites as a function of CNTs wt.%. Fracture toughness was measured by indentation as well as single-edge V-notch beam method.



**Fig. 4.** Creep strain recorded as a function of time (a) and creep rate as a function of creep strain measured during compression creep test for composites with different amounts of CNTs.

interestingly, with further addition of MWCNTs (e.g. 3 or 5 wt.%), after a transient creep during a few minutes, true strain reaches a constant value. The variation of zirconia grain sizes with different amounts of nanotubes (Table 1) evidences that such creep reduction is effectively due to MWCNTs. Opposite to common behavior of ceramics at high temperature, the specimen with smallest grain size (highest MWCNT content) shows the lowest creep. The reason for the higher creep resistance in finer structures is the effective presence of MWCNTs pinning grain boundaries at high temperature.

Another look on the creep performance of nanocomposite is represented in Fig. 4b. Obviously, the creep rate decreases with increasing nanotube percentage. This result is in line with previous findings reported by Zapata-Solvas [11] for alumina-10 vol.% single-walled CNT nanocomposites. Almost steady state creep is obtained for 3YSZ and 3YSZ reinforced with 0.5 wt.% MWCNT but the latter shows a lower creep rate than monolithic zirconia. For nanocomposites with higher amount of MWCNTs (1.5, 3 and 5 wt.%) after a transient decreasing creep, the creep rate drops to almost zero. For instance, in 3YSZ reinforced with 5 wt.% MWCNTs, the creep rate decreased three orders of magnitudes after a strain of only 0.07. From a microscopic point of view, this behavior can be interpreted as follow. At the onset of creep, strain is probably

due to slight rearrangement of grains to reach a relaxed status. As strain increases, the MWCNTs entangle and the creep rate strongly decreases to almost zero (Fig. 4b).

Fig. 5a and b shows the variation of mechanical loss  $\tan(\phi)$  [38] and relative shear modulus as a function of temperature for composites with different amounts of MWCNT in comparison with monolithic zirconia. As previously observed in zirconia [39], the spectra are characterized by an exponential increase in mechanical loss at temperature above 1250 K in the monolithic sample, accompanied by a steep decrease in the shear modulus [39]. The exponential increase in  $\tan(\phi)$  has been associated with the right shoulder of a grain boundary sliding peak, located at temperature higher than 1600 K at 1 Hz [2,39]. Clearly, the presence of MWCNTs shifts the exponential increase at higher temperature, e.g. for 3YSZ/5 wt.%MWCNT it starts at about 1400 K. Another interesting point to notice in Fig. 5b is the higher shear modulus of 3YSZ/MWCNTs nanocomposite in comparison with monolithic zirconia in the whole range of testing temperature, which is in agreement with the results of the modulus measured at room temperature (Table 2). Daraktchiev et al. [13] showed higher mechanical loss of monolithic zirconia in comparison with zirconia-CNTs composite, but their HR-TEM analysis have revealed that conventional sintering at 1723 K for 3 h could not preserve nanotubes,

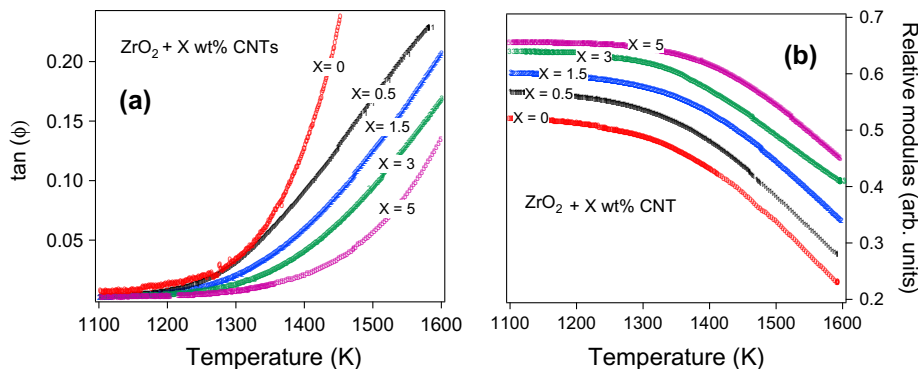


**Fig. 5.** Mechanical loss ( $\tan(\phi)$ ) and relative shear modulus as a function of temperature for zirconia/CNTs nanocomposites in comparison with monolithic zirconia. The measurement frequency was 1 Hz.

**Table 2**

Shear modulus of sintered 3YSZ/MWCNTs nanocomposites with various amounts of MWCNTs in comparison with monolithic zirconia.

Material composition	Shear modulus (GPa)
3YSZ	$78 \pm 6.5$
3YSZ/0.5 wt.% CNT	$82 \pm 5.4$
3YSZ/1.5 wt.% CNT	$92 \pm 4.3$
3YSZ/3 wt.% CNT	$99 \pm 3.8$
3YSZ/5 wt.% CNT	$107 \pm 3.8$

leading to formation of amorphous carbon at the grain boundaries. Therefore, CNTs pinning efficiency in their composites was much less than that of the present work [13].

#### 4. Discussion

Referring to open literature [12,13,17–19,21,32,40–42] on mechanical properties reported for zirconia ceramics reinforced by CNTs, the results presented here show a synergetic effect of CNTs on structural and functional properties of zirconia ceramic in a wide range of working temperature (25–1400 °C) for the first time. Often it is not easy to improve both toughness and creep resistance. In the present study, we show that introducing MWCNTs in polycrystalline nanograin zirconia, leads to a significant increase in fracture toughness and creep resistance. The dual role of MWCNTs in toughening and creep resistance of nanograin zirconia could be explained as following.

As seen in Fig. 3, a significant increase in indentation fracture toughness and a slight hardness improvement are observed with the addition of 5 wt.% (12.5 vol.%) MWCNTs. This can be attributed to the extent of interfacial bonding between MWCNTs and zirconia grains formed during SPS and to the survival of CNTs after consolidation [24]. The excellent interfacial bonding between CNTs and zirconia, is proven by the increase in the modulus of reinforced ceramics in comparison with the monolithic ones (see Table 2). The shear modulus reaches 107 GPa for zirconia reinforced with 5 wt.% (~12.5 vol.%) of MWCNTs showing a 38% increase in comparison with monolithic zirconia. Fracture toughness measured by indentation in ceramics reinforced by CNTs has been matter of dispute [23,25]. Indentation is an indirect toughness-testing technique in shear mode, whereas the crack tip in fracture toughness measurement should be subjected to mode I tension. Wang et al. [23] showed that even if the indentation fracture toughness of alumina reinforced by CNTs is higher than that of monolithic alumina, their single edge V-notched beam (SEVNB) fracture toughness results did not demonstrate a significant difference. This is an argument to be taken into consideration when making

fracture toughness assessment. To have a better insight on the effect of MWCNTs on fracture toughness under tension, we also measured fracture toughness of 3YSZ/MWCNTs nanocomposite in bending tests. Although the increase in fracture toughness is not as high as in tests obtained by the indentation method, it is significant (Fig. 3a). To the best of our knowledge, the present result is the first report that shows an improvement in fracture toughness of zirconia/MWCNTs under bending stress. The homogenous distribution of high amounts (~12.5 vol.%) of MWCNTs (Fig. 2a and b), the survival of MWCNTs after SPS consolidation (Fig. 2c), the extended bonding between CNTs and zirconia grains and the high density of SPS samples (Table 1) resulted in high fracture toughness of nanocomposites. Cha et al. [43] have employed molecular level mixing (MLM) to fabricate  $\text{Al}_2\text{O}_3$ /CNTs nanocomposite to produce homogeneously dispersed CNTs in  $\text{Al}_2\text{O}_3$  powder. However, the hardness decreased with an increase in the CNT volume fraction beyond 2 vol.% because of CNT agglomeration. On the contrary, the present study shows a continuous increase in fracture toughness and hardness with CNT content up to 12.5 vol.%.

To distinguish the effect of phase transformation toughening [44] from the effect of MWCNTs on fracture toughness, the amount of stress-induced monoclinic phase on fracture surface was determined by XRD analysis (Fig. 3d). Interestingly, a continuous decrease of stress-induced monoclinic phase with the increase of MWCNTs content is obtained. Thus, a higher fracture toughness of nanocomposite must not have been resulted from transformation toughening and can only be attributed to nanotubes. The decreasing content of monoclinic phase in the composites with higher amount of MWCNTs is probably due to their smaller grain sizes. It is recognized that the propensity to undergo the transformation decreases with the reduction of zirconia grain size [45,46].

It was frequently reported that in fiber-reinforced composite, fiber pull-out, crack deflection and crack bridging are the most effective toughening mechanisms [14,24,47–51]. Fig. 6 shows a SEM picture of indentation-induced crack on the surface of 3YSZ/5 wt.%MWCNTs. The MWCNTs are stretched between crack faces, which shows crack bridging (Fig. 6b and c). Crack deflection (Fig. 6a) and MWCNTs pull-out (Fig. 6b) can also be seen.

The above mentioned mechanisms are among possible classical toughening mechanisms of conventional ceramic composites reinforced by fibers and whiskers [52]. Although these mechanisms were mentioned several times as forceful ones to explain toughening in CNT–ceramic composites [47–50], there is a clear difference between fiber-reinforced and CNT-reinforced ceramics [26]. It has been demonstrated that conventional fiber–ceramic composites show a compromise between toughness and strength [26,52,53]. The fibers can bridge the crack in its wake and are pulled out as the crack advances, which dissipates energy and increases the

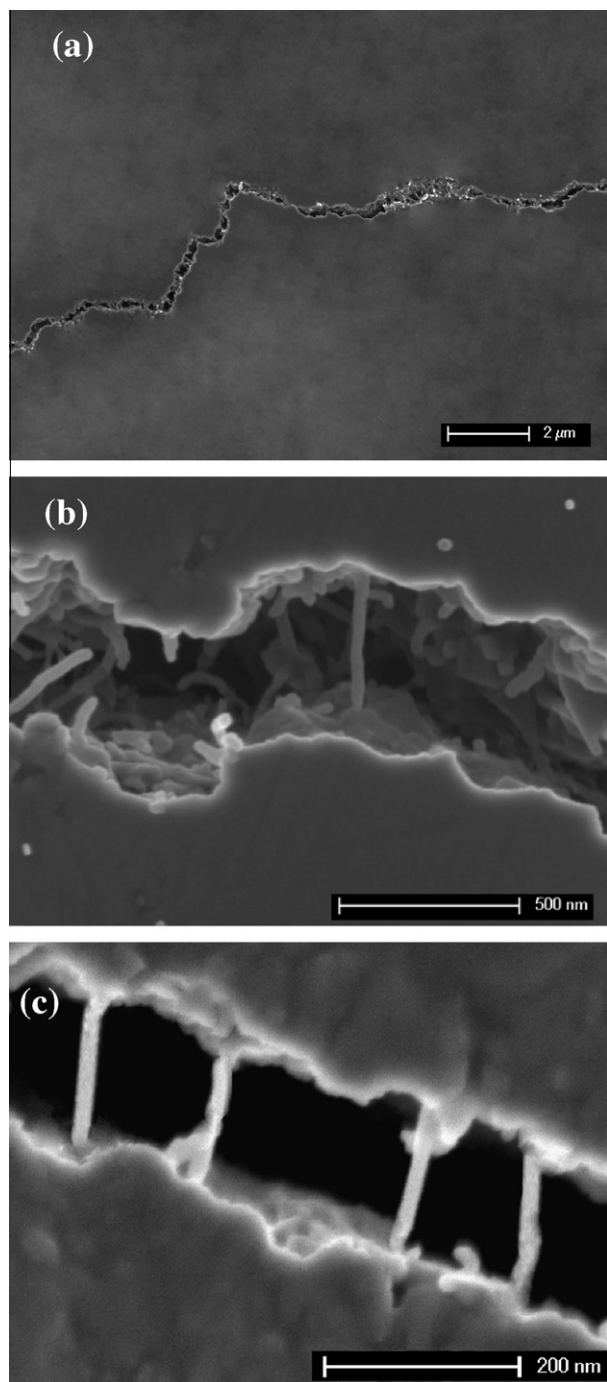


**Fig. 6.** SEM picture of indentation-induced crack on the surface of 3YSZ/5 wt.% MWCNTs shows different toughening mechanism.

toughness [52]. In a downside, large fibers also produce large flaws, which in turn result in lower hardness and strength [26]. In the present system, instead, we observe a simultaneous improvement in fracture toughness and hardness. Moreover, the classical fiber pull-out toughening mechanisms of traditional fibers/whiskers composites should be absent in the present CNT-composites for two reasons. (1) The conventional composites usually contain straight fibers, with a diameter larger than or equal to ceramic grain size (several micrometers) and with a length of several hundreds of micrometers. Instead, nanotubes that are flexible because of the high aspect ratio are not embedded within the ceramic grains like fibers and lie essentially at grain boundaries. Therefore,

they are not expected to give raise to a fiber pull-out toughening mechanism. The short length of emerging CNTs (<200 nm) at fracture surface supports this hypothesis, as evidenced by Todd and his coworkers [49] energy dissipation produced by few nanometers (~100 nm) debonding of randomly oriented MWCNTs is negligible. (2) The interface between fiber and matrix has to be optimally designed [26,52]. A rather weak interface is needed in order to allow for fiber pull-out, which produces energy dissipation by friction, and consequently toughening [53]. However, in the present CNT-ceramic composite, the shear modulus measurements (Table 2) and HR-TEM observation (Fig. 2c) indicate that we have a strong interface, which does not allow pull-out.

Another possible mechanism in CNT-ceramic composite, which could explain both toughening and strengthening is uncoiling and stretching of nanotubes [26]. When the crack propagates intergranularly, the entangled nanotubes bundles are uncoiled in the first step. With further propagation of crack, the uncoiled nanotubes would stretch, while their end is anchored within the grains. Fig. 6c shows these stretched nanotubes, which produce crack bridging. With further propagation of crack, the nanotubes will separate from ceramic interface or fail (Figs. 2a and 6b). The uncoiling/stretching produces friction work and dissipates energy at the crack tip, which results in higher toughness. Moreover, nano-scale CNTs would produce smaller or no flaws relative to conventional fiber and whiskers.

High temperature mechanical tests of zirconia/MWCNTs nanostructured composites show a significant reduction of plastic strain in the presence of MWCNTs (Fig. 4) while monolithic zirconia exhibits superplastic deformation. This is consistent [54] with the remarkable decrease of mechanical loss in the presence of CNTs (Fig. 5). While, diffusional creep and grain boundary sliding (GBS) are the dominant deformation mechanisms in zirconia at high temperatures, the higher creep resistance of the present nanocomposite can result from a pinning effect of CNTs blocking GBS (Fig. 5b). A theoretical model was developed by Lakki et al. [39] to investigate the role of material stiffness on the presence of microcreep in ceramics. The model accounts for relative sliding of hexagonal grains separated by a viscous layer [39]. When a shear stress is applied on the grains, two forces are generated at the boundary. (1) A dissipative force due to the viscosity of the sliding intergranular layer and (2) a restoring force opposing sliding due to geometric constraint of neighboring grains. The restoring force at triple junctions strongly reduces with temperature and fully disappears at high temperature due to diffusion [39]. Strain is no more limited and consequently the mechanical loss increases exponentially [2,54]. Such an exponential increase in mechanical loss can be correlated to the beginning of creep (Fig. 5a). The presence of the CNTs at grain boundaries can provide an additional restoring force that is not temperature dependent. Therefore, creep is decreased or suppressed and anelastic strain that is measured by mechanical spectroscopy is strongly reduced or delayed to higher temperature (Fig. 5a).

## 5. Conclusion

SPS consolidation of zirconia with MWCNT addition allows the production of ceramic nanocomposites with enhanced mechanical properties both at room and high temperature (creep resistance, hardness, toughness and shear modulus), and high electrical conductivity. These performances are due to new toughening mechanism as a result of the embedment of CNT at grain boundaries and to the ability of CNT to inhibit grain boundary sliding and creep at high temperature. The base material presented in this paper represents a promising candidate for novel multifunctional applications.



## Acknowledgement

The Swiss National Foundation is acknowledged for financial support.

## References

- [1] Fantozzi G, Chevalier J, Olagnon C, Chermant JL, Anthony K, Carl Z. Creep of ceramic matrix composites. *Comprehensive composite materials*, Oxford: Pergamon; 2000. p. 115–62.
- [2] Schaller R, Lakki A. Grain boundary relaxations in ceramics. *Mater Sci Forum* 2001;366–368:315–37.
- [3] Wakai F, Sakaguchi S, Matsuno Y. Superplasticity of yttria-stabilized tetragonal ZrO<sub>2</sub> polycrystals. *Adv Ceram Mater* 1986;1(3):259–63.
- [4] Raj R, Ashby MF. On grain boundary sliding and diffusional creep. *Metall Mater Trans B* 1971;2(4):1113–27.
- [5] Maehara Y, Langdon TG. Superplasticity in ceramics. *J Mater Sci* 1990;25(5):2275–86.
- [6] Thompson AM, Chan HM, Harmer MP. Tensile creep of alumina-silicon carbide “nanocomposites”. *J Am Ceram Soc* 1997;80(9):2221–8.
- [7] Ohji T, Nakahira A, Hirano T, Niihara K. Tensile creep behavior of alumina/silicon carbide nanocomposite. *J Am Ceram Soc* 1994;77(12):3259–62.
- [8] Ohji T, Kusunose T, Niihara K. Threshold stress in creep of alumina-silicon carbide nanocomposites. *J Am Ceram Soc* 1998;81(10):2713–6.
- [9] Lin H-T, Becher PF. Creep behavior of a SiC-whisker-reinforced alumina. *J Am Ceram Soc* 2005;73(5):1378–81.
- [10] Baughman RH, Zakhidov AA, De Heer WA. Carbon nanotubes – the route toward applications. *Science* 2002;297(5582):787–92.
- [11] Zapata-Solvas E, Poyato R, Gómez-García D, Domínguez-Rodríguez A, Radmilovic V, Padture NP. Creep-resistant composites of alumina and single-wall carbon nanotubes. *Appl Phys Lett* 2008;92(11).
- [12] Mazaheri M, Mari D, Schaller R. High temperature mechanical spectroscopy of yttria stabilized zirconia reinforced with carbon nanotubes. *Phys Status Solidi (a)* 2010;207(11):2456–60.
- [13] Daraktchiev M, Van De Moorte B, Schaller R, Couteau E, Forro L. Effects of carbon nanotubes on grain boundary sliding in zirconia polycrystals. *Adv Mater* 2005;17(1):88–91.
- [14] Curtin WA, Sheldon BW. CNT-reinforced ceramics and metals. *Mater Today* 2004;7(11):44–9.
- [15] Cho J, Boccaccini AR, Shaffer MSP. Ceramic matrix composites containing carbon nanotubes. *J Mater Sci* 2009;44(8):1934–51.
- [16] Flahaut E, Peigney A, Laurent C, Marlière C, Chastel F, Rousset A. Carbon nanotube-metal-oxide nanocomposites: microstructure, electrical conductivity and mechanical properties. *Acta Mater* 2000;48(14):3803–12.
- [17] Duszka J, Blugan G, Morgiel J, Kuebler J, Inam F, Peijs T, et al. Hot pressed and spark plasma sintered zirconia/carbon nanofiber composites. *J Eur Ceram Soc* 2009;29(15):3177–84.
- [18] Duszova A, Duszka J, Tomasek K, Morgiel J, Blugan G, Kuebler J. Zirconia/carbon nanofiber composite. *Scripta Mater* 2008;58(6):520–3.
- [19] Sun J, Gao L, Iwasa M, Nakayama T, Niihara K. Failure investigation of carbon nanotube/3Y-TZP nanocomposites. *Ceram Int* 2005;31(8):1131–4.
- [20] Zapata-Solvas E, Gómez-García D, Poyato R, Lee Z, Castillo-Rodríguez M, Domínguez-Rodríguez A, et al. Microstructural effects on the creep deformation of alumina single-wall carbon nanotubes composites. *J Am Ceram Soc* 2008;93(7):2042–7.
- [21] Zhou JP, Gong QM, Yuan KY, Wu JJ, Chen Yf, Li CS, et al. The effects of multiwalled carbon nanotubes on the hot-pressed 3 mol% yttria stabilized zirconia ceramics. *Mater Sci Eng A* 2009;520(1–2):153–7.
- [22] Peigney A, García FL, Estournès C, Weibel A, Laurent C. Toughening and hardening in double-walled carbon nanotube/nanostructured magnesia composites. *Carbon* 2010;48(7):1952–60.
- [23] Wang X, Padture NP, Tanaka H. Contact-damage-resistant ceramic/single-wall carbon nanotubes and ceramic/graphite composites. *Nat Mater* 2004;3(8):539–44.
- [24] Zhan GD, Kuntz JD, Wan J, Mukherjee AK. Single-wall carbon nanotubes as attractive toughening agents in alumina-based nanocomposites. *Nat Mater* 2003;2(1):38–42.
- [25] Sheldon BW, Curtin WA. Nanoceramic composites: tough to test. *Nat Mater* 2004;3(8):505–6.
- [26] Padture NP. Multifunctional composites of ceramics and single-walled carbon nanotubes. *Adv Mater* 2009;21(17):1767–70.
- [27] Mazaheri M, Valefi M, Hesabi ZR, Sadmezhad SK. Two-step sintering of nanocrystalline 8Y<sub>2</sub>O<sub>3</sub> stabilized ZrO<sub>2</sub> synthesized by glycine nitrate process. *Ceramics International* 2009;35(1):13–20.
- [28] Anstis GR, Chantikul P, Lawn BR, Marshall DB. A critical evaluation of indentation techniques for measuring fracture toughness: I, direct crack measurements. *J Am Ceram Soc* 1981;64(9):533–8.
- [29] Kubler J. Fracture toughness of ceramics using the SEVNB method from a preliminary study to a standard test method. In: Salem JA, Quinn GD, Jenkins MG, editors. *Fracture resistance testing of monolithic and composite brittle*. West Conshohocken, Pennsylvania: American Society for Testing and Materials; 2002. p. 93–106.
- [30] Mazaheri M, Mari D, Schaller R, Bonnefont G, Fantozzi G. Processing of yttria stabilized zirconia reinforced with carbon nanotubes with attractive mechanical properties. *J Eur Ceram Soc*; 2011. doi:10.1016/j.jeurceramsoc.2010.11.009.
- [31] Daraktchiev M, Schaller R. High-temperature mechanical loss behaviour of 3 mol% yttria-stabilized tetragonal zirconia polycrystals (3Y-TZP). *Phys Status Solidi (A)* Appl Res 2003;195(2):293–304.
- [32] Duszová A, Duszka J, Tomášek K, Blugan G, Kuebler J. Microstructure and properties of carbon nanotube/zirconia composite. *J Eur Ceram Soc* 2008;28(5):1023–7.
- [33] Vasiliev AL, Poyato R, Padture NP. Single-wall carbon nanotubes at ceramic grain boundaries. *Scripta Mater* 2007;56(6):461–3.
- [34] Liu M, Cowley JM. Structures of the helical carbon nanotubes. *Carbon* 1994;32(3):393–403.
- [35] Shi SL, Liang J. Effect of multiwall carbon nanotubes on electrical and dielectric properties of yttria-stabilized zirconia ceramic. *J Am Ceram Soc* 2006;89(11):3533–5.
- [36] Menchavez RL, Fuji M, Takahashi M. Electrically conductive dense and porous alumina with in situ-synthesized nanoscale carbon networks. *J Am Ceram Soc* 2008;20(12):2845–51.
- [37] Tatami J, Katashima T, Komeya K, Meguro T, Wakihara T. Electrically conductive CNT-dispersed silicon nitride ceramics. *J Am Ceram Soc* 2005;88(10):2889–93.
- [38] Schaller R, Daraktchiev M, Testu S. Creep behavior of ceramics studied by mechanical loss measurements. *Mater Sci Eng A* 2004; 387–389(1–2 SPEC. ISS.) 687–91.
- [39] Lakki A, Schaller R, Nauer M, Carry C. High temperature superplastic creep and internal friction of yttria doped zirconia polycrystals. *Acta Metall Et Mater* 1993;41(10):2845–53.
- [40] Garmendia N, Santacruz I, Moreno R, Obieta I. Slip casting of nanozirconia/MWCNT composites using a heterocoagulation process. *J Eur Ceram Soc* 2009;29(10):1939–45.
- [41] Ukai T, Sekino T, Hirvonen A, Tanaka N, Kusunose T, Nakayama T, et al. Preparation and electrical properties of carbon nanotubes dispersed zirconia nanocomposites. *Key Eng Mater* 2006;317–318:661–4.
- [42] Datye A, Wu K-H, Gomes G, Monroy V, Lin H-T, Vleugels J, et al. Synthesis, microstructure and mechanical properties of Yttria Stabilized Zirconia (3YTZP) – Multi-Walled Nanotube (MWNTs) nanocomposite by direct in situ growth of MWNTs on Zirconia particles. *Compos Sci Technol* 2010;70(14):2086–92.
- [43] Cha SI, Kim KT, Lee KH, Mo CB, Hong SH. Strengthening and toughening of carbon nanotube reinforced alumina nanocomposite fabricated by molecular level mixing process. *Scripta Mater* 2005;53(7):793–7.
- [44] Lange FF. Transformation toughening. *J Mater Sci* 1982;17(1):225–34.
- [45] Becher PF, Swain MV. Grain-size-dependent transformation behavior in polycrystalline tetragonal zirconia. *J Am Ceram Soc* 1992;75(3):493–502.
- [46] Suresh A, Mayo MJ, Porter WD, Rawn CJ. Crystallite and grain-size-dependent phase transformations in yttria-doped zirconia. *J Am Ceram Soc* 2003;86(2):360–2.
- [47] Ahmad I, Cao H, Chen H, Zhao H, Kennedy A, Zhu YQ. Carbon nanotube toughened aluminium oxide nanocomposite. *J Eur Ceram Soc* 2010;30(4):865–73.
- [48] Corral EL, Cesarano Iii J, Shyam A, Lara-Curzio E, Bell N, Stuecker J, et al. Engineered nanostructures for multifunctional single-walled carbon nanotube reinforced silicon nitride nanocomposites. *J Am Ceram Soc* 2008;91(10):3129–37.
- [49] Mukhopadhyay A, Chu BTT, Green MLH, Todd RI. Understanding the mechanical reinforcement of uniformly dispersed multiwalled carbon nanotubes in alumino-borosilicate glass ceramic. *Acta Mater* 2010;58(7):2685–97.
- [50] Xia Z, Riester L, Curtin WA, Li H, Sheldon BW, Liang J, et al. Direct observation of toughening mechanisms in carbon nanotube ceramic matrix composites. *Acta Mater* 2004;52(4):931–44.
- [51] Fan JP, Zhuang DM, Zhao DQ, Zhang G, Wu MS, Wei F, et al. Toughening and reinforcing alumina matrix composite with single-wall carbon nanotubes. *Appl Phys Lett* 2006;89(12).
- [52] Green DG. An introduction to the mechanical properties of ceramics. Cambridge, UK: Cambridge University Press; 1998.
- [53] Harris B, Anthony K, Carl Z. Long-fiber-reinforced dense glass-and ceramic-matrix composites. *Comprehensive composite materials*, Oxford: Pergamon; 2000. p. 489–531.
- [54] Schaller R, Daraktchiev M. Mechanical spectroscopy of creep appearance in fine-grained yttria-stabilized zirconia. *J Eur Ceram Soc* 2002;22(14–15):2461–7.